

Effect of Dopant on the Morphological and Electrical Properties of Polyaniline/MCM-41 Nanocomposites

SADIA AMEEN^{1,†}, M. HUSAIN², M. SHAHEER AKHTAR³, YOUNG SOON KIM^{1,†} and HYUNG-SHIK SHIN^{1,*}

¹Energy Materials & Surface Science Laboratory, Solar Energy Research Center, School of Chemical Engineering, Chonbuk National University, Jeonju 561-756, Republic of Korea

²Department of Physics, Jamia Millia Islamia, Jamia Nagar, New Delhi-110 025, India

³New & Renewable Energy Material Development Center, Chonbuk National University, Buan-gun, Jeonbuk, Republic of Korea

*Corresponding author: Fax: +82 63 2702306; Tel: +82 63 2704318; E-mail: hsshin@jbnu.ac.kr

†Authors contributed equally to this work.

(Received: 20 February 2010;

Accepted: 24 September 2010)

AJC-9122

The novel organic-inorganic nanocomposite was prepared with polyaniline (PANI) and mesoporous MCM-41 by the polymerization of aniline hydrochloride monomer. The structural, crystalline and Raman results confirmed the formation of the nanocomposites through the interaction between PANI molecules and MCM-41. DC conductivity of the nanocomposites was significantly affected by the incorporation of HCl doped PANI molecules into PANI/MCM-41 nanocomposites. It was observed that the undoped polyaniline/MCM-41 nanocomposite presented an electrically insulating DC conductivity of the order of $10^{-13} \text{ ohm}^{-1} \text{ cm}^{-1}$ and after the introduction of HCl doped PANI molecules into MCM-41, the proton conductivity reached the order of $10^{-3} \text{ ohm}^{-1} \text{ cm}^{-1}$.

Key Words: Mesoporous material, Electrical conductivity, Organic-inorganic nanocomposite, Polyaniline.

INTRODUCTION

Mesoporous materials are of great interest because of their potential applications in the various research fields that traverses from catalysis to drug delivery^{1,2}. Recently, the surface modification of mesoporous molecular sieves are employed as proton conducting solid materials and of great interest due to their potential applications in electrochemical devices, such as batteries and fuel cells^{3,4}. Polyaniline (PANI) is widely studied conducting polymer with effective applications in electromagnetic shielding, rechargeable batteries, light emitting diodes, non-linear optical devices, sensors for medicine and as membranes for the separation of gas mixtures^{5,6}. Several groups have reported that a thermal stability of PANI could be improved by combining PANI with polystyrene latex⁷, multi-walled carbon nanotubes⁸, ZnO nanomaterials⁹, montmorillonite¹⁰, graphite¹¹ and mesoporous silica (MCM-41)¹²⁻¹⁴. Out of these, MCM-41 has recently attracted the attention as a promising material for catalysts and could be used in the industrial processes such as adsorption, ion exchange and environmental control¹⁵.

So far, studies based on the PANI/MCM-41 nanocomposites have been performed for electrorheological properties¹⁶, thermal stability¹⁷ and to study the various polymerization techniques for the preparation of PANI/MCM-41 nanocomposites¹⁸. To the best of our knowledge, none of the studies,

related to the doping of PANI/MCM-41 nanocomposites has been reported yet. This study presents the doping effects, characterizations and the DC conductivity measurements of PANI/MCM-41 nanocomposites. The synthesis of the nanocomposite is accomplished by the polymerization of aniline hydrochloride monomer with MCM-41. The DC conductivity increases from insulating to the conducting range upon protonic (HCl) doping. The interaction of MCM-41 with PANI molecules is confirmed by the effective morphological and structural characterizations.

EXPERIMENTAL

Synthesis of PANI/MCM-41 nanocomposites: The desired chemicals for the preparation of MCM-41 are listed as tetraethyl orthosilicate (TEOS, Aldrich-Sigma), cetyltrimethylammonium bromide (CTAB, Aldrich-Sigma), Hydrochloric acid (35 %, Aldrich-Sigma), methanol (99 %, Shanchun chemical) and deionized water (DI). The preparation of MCM-41 was performed with the molar composition of TEOS/H₂O/HCl/MeOH/CTAB = 1:5.2: 0.06:5:0.25. The synthesized MCM-41 was calcined at 500 °C with ramp speed of 1 °C/min for burning the residual organic materials.

For the synthesis of PANI/MCM-41 nanocomposites, the fixed amount (0.2 g) of MCM-41 was mixed in a solution containing aniline hydrochloride (0.2 g) and 10 mL of methanol.

The reaction mixture was stirred for a few minutes for the dispersion of MCM-41 and then allowed to dry at room temperature. Further, the aniline/MCM-41 powder was dispersed in fixed amount of 20 mL of 0.02 N HCl. To this mixture, a solution of 0.35 g of ammonium peroxydisulphate (APS), taken in 10 mL of 0.02 N HCl was added and subjected to stirring at room temperature for 12 h. The obtained PANI/MCM-41 nanocomposite was stirred in 0.05 M NH_4OH to achieve emeraldine base (EB) from green emeraldine salt (ES) and then filtered and washed thoroughly with deionized water and later kept for drying at 50 °C. The obtained dark blue powder was stirred with different percentage (%) of 0.02 N HCl (dopant) for studying the doping effect on the synthesized PANI/MCM-41 nanocomposites.

Characterizations: The morphological observations of PANI/MCM-41 nanocomposite were observed using field emission scanning electron microscopy (FESEM, Hitachi S-4700, Japan). Information about the crystallinity was obtained by the X-rays diffraction (XRD, Rigaku, $\text{CuK}\alpha$, $\lambda = 1.54178 \text{ \AA}$). The structural characterizations of PANI/MCM-41 nanocomposite were prevailed through Raman spectroscopy (Raman microscope, Renishaw). For DC conductivity measurements (σ_{dc}), the voltage of 1.5 V (from regulated supply) was applied across the samples (pellets) and the resulting current was measured with a Keithley electrometer (model-617).

RESULTS AND DISCUSSION

Fig. 1 shows the FESEM images of MCM-41 and PANI/MCM-41 nanocomposites. The image presents agglomerates of PANI/MCM-41 nanocomposites. As the dopant ratio is increases, the morphology dramatically changes to smaller well defined shapes and possibly exhibits debris like structures. However, no difference has been observed in the surface morphology of the pristine MCM-41 [Fig. 1(a)] and the PANI/MCM-41 nanocomposites [Fig. 1 (b)]. The smaller debris shaped morphology of PANI/MCM-41 nanocomposites might due to the interaction of PANI molecules with MCM-41, as shown in Fig. 1(d).

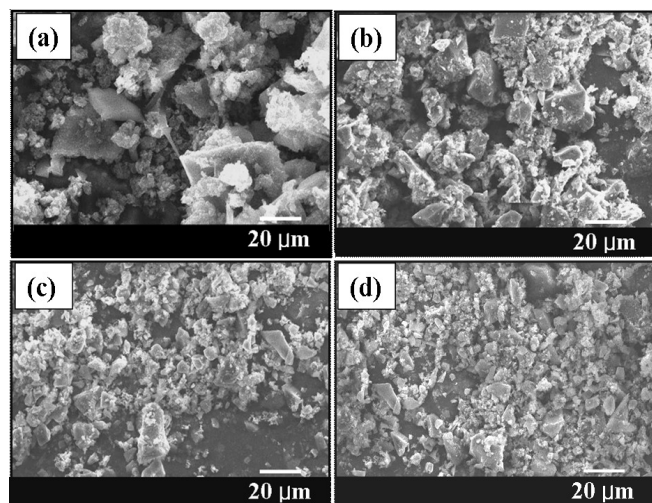


Fig. 1. FESEM images of the (a) pristine MCM-41 (b) PANI/MCM-41 nanocomposite with 2% dopant (c) PANI/MCM-41 nanocomposite with 8% dopant (d) PANI/MCM-41 nanocomposite with 10% dopant

The XRD patterns of the PANI/MCM-41 nanocomposites with different concentration of dopant are almost identical to each other, as presented in Fig. 2. The existence of the peak at *ca.* 23° is the characteristic peak of PANI and is ascribed to the periodicity parallel and perpendicular to the polymer (PANI) chain. The intensity of this prominent peak increases with the increased concentration of dopant into the PANI/MCM-41 nanocomposite. This increase in intensity of the peak favours the enhanced crystallinity of the PANI/MCM-41 nanocomposites as compared to MCM-41.

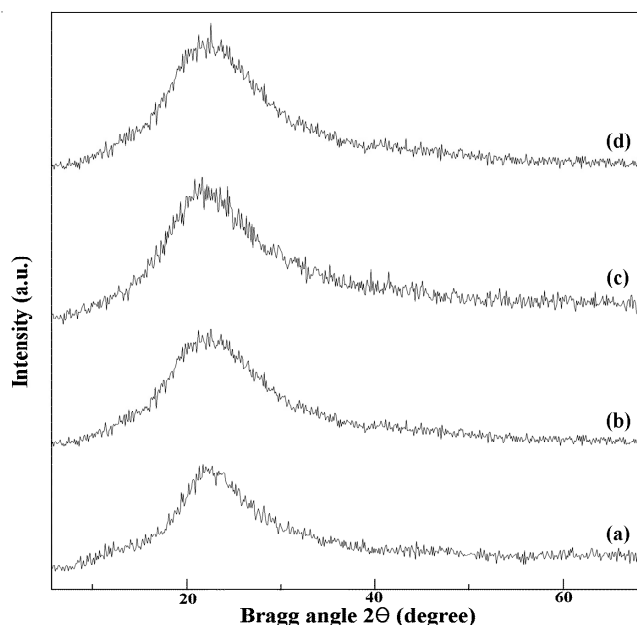


Fig. 2. XRD patterns of (a) 2%, (b) 4%, (c) 8% and (d) 10% doped PANI/MCM-41 nanocomposites

The appearance of different peaks of the HCl doped PANI/MCM-41 nanocomposites could be seen in Raman spectra as depicted in Fig. 3. It uniquely indicates the presence of the PANI emeraldine salt (ES) structure in the nano-composite. In 2% doped PANI/MCM-41 nanocomposites, the appearance

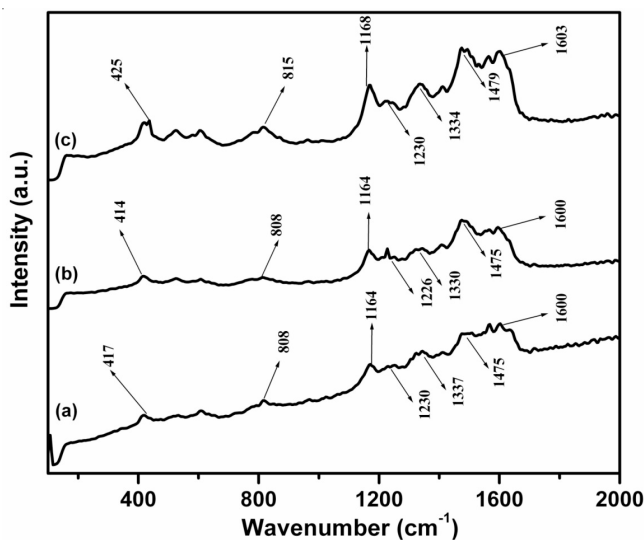


Fig. 3. Raman spectra of (a) 2%, (b) 4% and (c) 10% doped PANI/MCM-41 nanocomposites

of peaks at around 330, 1164, 1230, 1475 and 1600 cm^{-1} are related to PANI and correspond to the C-N stretching, C-H bending of the quinoid ring, C-H bending of the benzenoid ring and C-C stretching of the benzenoid ring, respectively [Fig. 3(a)]. The peak at 808 cm^{-1} ascribes the symmetric Si-O-Si stretching and the peak at 414 cm^{-1} represents Si-O-Si bending in nanocomposite. The increase in the concentration of the dopant changes the peak intensity and the position of the peaks. This indicates a strong interaction between doped PANI molecules and MCM-41. These results are consistent with FESEM and XRD data and show that the dopant concentration is crucial to prepare advanced PANI/MCM-41 nanocomposites.

In order to investigate the DC conductivity, nanocomposite samples with diameter and thickness of 1.01 and 0.016 cm, respectively were prepared in the form of pellets. These pellets were placed between the two steel electrodes, situated inside a metallic sample holder for the conductivity measurements. Two-point probe conductivity was measured in the temperature range of 300-400 K and is given by the following relation

$$\sigma_{dc} = \sigma_0 \exp(-\Delta E/kT)$$

where ΔE = activation energy, k = Boltzmann constant and σ_0 is the pre-exponential factor. The plotting of a graph between $\ln \sigma$ and $1000/T$, shown in Fig. 4(a), exhibits a straight line of slope $(\Delta E/1000 \text{ K})$ and intercept $\ln \sigma_0$. From Fig. 4(b), the DC conductivity increases with the increase of dopant concentration into the nanocomposites. The calculated values of DC conductivity and other related parameters of the nanocomposites, prepared from different concentration of dopant are summarized in Table-1. Proton conductivity in the mesoporous materials is achieved by preparing mesoporous compositions that generate negatively charged frameworks which could be charge balanced by protons. In present case, the increase in conductivity of PANI/MCM-41 nanocomposite is credited to the strong interaction of dopant molecule to PANI molecule with mesoporous MCM-41. It has been reported that emeraldine salt is partially crystalline and emeraldine base is partially amorphous in nature¹⁹. In PANI/MCM-41 nanocomposite, the presence of dopant increases the crystallinity and therefore, facilitates the movement of the charge carriers. The attraction of an electron in one repeated unit to the nuclei of other neighboring unit leads the charge carrier delocalization and thus, increases the carrier mobility along the PANI chain which constitutes the nanocomposite. The energy required for the transition state from the defect states to the valence or the conduction band has not been changed much and ultimately the value of ΔE does not change significantly. However, a sharp increase in the value of ΔE for 6 % doped PANI/MCM-41 nanocomposites might due to the decrease in the density of the localized states in the mobility gap of PANI. The conduction mechanism has been explained by Mott and Davis model. According to Mott and Davis²⁰, the value of σ_0 in the range of 10^3 - $10^4 \text{ ohm}^{-1} \text{ cm}^{-1}$ indicates that the conduction is mostly in the extended states. The smaller value of σ_0 indicates wide range of localized states and the conduction by hopping process where a still smaller value of σ_0 (negatives values) shows that conduction is taking place through hopping process due to the

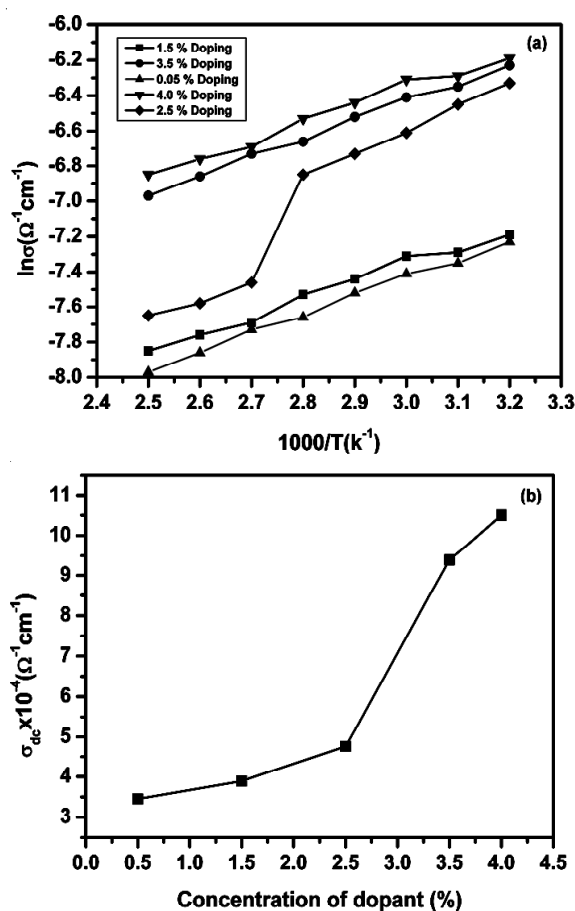


Fig. 4. (a) Variation of $\ln \sigma$ versus $1000/T$ (b) Conductivity versus different concentration of dopant (%) of PANI/MCM-41 nanocomposites

TABLE-1
ELECTRICAL PARAMETERS OF PANI/MCM-41
NANOCOMPOSITES WITH DIFFERENT CONCENTRATION OF
DOPANT (%) AT TEMPERATURE 330 K

Composites	Conductivity parameters		
	DC conductivity (σ_{dc}) ($\Omega^{-1} \text{ cm}^{-1}$)	Pre-exponential factor (σ_0) ($\Omega^{-1} \text{ cm}^{-1}$)	Activation energy ($\Delta E \times 10^{-2}$) (eV)
PANI/MCM-41	2.70×10^{-13}	4.28×10^{-10}	20.0
2 % HCl doped PANI/MCM-41	3.45×10^{-4}	8.31×10^{-3}	9.04
4 % HCl doped PANI/MCM-41	3.89×10^{-4}	7.37×10^{-3}	8.35
6 % HCl doped PANI/MCM-41	4.76×10^{-4}	2.67×10^{-1}	18.0
8 % HCl doped PANI/MCM-41	9.39×10^{-4}	2.25×10^{-2}	9.04
10 % HCl doped PANI/MCM-41	1.05×10^{-3}	2.00×10^{-2}	8.35

presence of wide range of localized states near the Fermi level. In present case, the magnitude of σ_0 is in the range of 10^3 - $10^2 \text{ ohm}^{-1} \text{ cm}^{-1}$ which suggests that conduction in extended states is not possible and thus, the conduction is taking through hopping process due to wide range of localized states present near the Fermi level.

Conclusion

Novel organic-inorganic PANI-MCM-41 nanocomposites have been synthesized with different concentration of HCl

doped PANI molecules and MCM-41 through the polymerization technique using aniline hydrochloride monomer as a starting material. Raman results substantiate the appearance of emeraldine salt units in the nanocomposites and confirm the formation of PANI/MCM-41 nanocomposites. The morphological and the crystalline properties of the PANI/MCM-41 nanocomposites affected strongly with varied concentration of HCl dopant. DC measurements of the PANI/MCM-41 nanocomposites show proficient conductivity, resulting from the good interaction between the free electron pairs of the nitrogen atoms of the PANI molecule with MCM-41. The enhancement in conductivity is accomplished by varying the amount of dopant in the synthesized PANI/MCM-41 nanocomposite.

ACKNOWLEDGEMENTS

The grant of 20093020010090-12-3-010 is fully acknowledged.

REFERENCES

1. C.T. Kresge, M.E. Lenowicz, W.J. Roth, J.C. Vartul and J.S. Beck, *Nature*, **359**, 710 (1992).
2. J.F. Diaz and J.K.J. Balkus, *J. Mol. Catal. B: Enzym*, **2**, 115 (1996).
3. S. Inagaki, S. Guan, T. Ohsuna and O. Terasaki, *Nature*, **416**, 304 (2002).
4. W. Wang, W. Zhou and A. Sayari, *Chem. Mater.*, **15**, 4886 (2003).
5. J.S. Shin, J.H. Kim and I.W. Cheong, *Synth. Met.*, **151**, 246 (2005).
6. Y. Yu, B. Che, Z. Si, L. Li, W. Chen and G. Xue, *Synth. Met.*, **150**, 271 (2005).
7. B.H. Kim, J.H. Juang, S.H. Hong, J. Joo, J. Epstein, K. Mizoguchi, J.W. Kim and H.J. Choi, *Macromolecules*, **35**, 1419 (2002).
8. A.J. Milton and A.P. Monkman, *J. Phys. D: Appl. Phys.*, **26**, 1468 (1993).
9. C.G. Wu and T. Bein, *Stud. Surf. Sci. Catal.*, **84**, 2269 (1994).
10. P. Enzel and T. Bein, *J. Phys. Chem.*, **93**, 6270 (1989).
11. T. Bein, *Stud. Surf. Sci. Catal.*, **102**, 295 (1996).
12. Z.H. Wang, E.M. Scherr, A.G. MacDiarmid and A. Epstein, *J. Phys. Rev. B*, **45**, 4190 (1992).
13. A.G. MacDiarmid, *Synth. Met.*, **125**, 11 (2002).
14. R. Madathil, R. Parkesh, S. Ponrathnam and M.C.J. Large, *Macromolecules*, **37**, 2002 (2004).
15. A.A.M. Rogerio, V.G. Marcus, R. Joao and A.G. Ernesto, *Mater. Res.*, **2**, 173 (1999).
16. H.J. Choi, M.S. Cho and W.S. Ahn, *Synth. Met.*, **135**, 711 (2003).
17. H. Nur, N.A. Rahman, S. Endud and L.K. Wei, *Malays. Polym. J.*, **2**, 12 (2007).
18. N. Kuramoto and E.M. Genies, *Synth. Met.*, **68**, 191 (1995).
19. H.K. Chaudhari and D.D.S. Kelkar, *J. Appl. Polym. Sci.*, **62**, 18 (1996).
20. N.F. Mott and E.A. Davis, *Philos. Mag.*, **2**, 7 (1970).

FUNCTIONAL GENOMICS - NEXT GENERATION APPLICATIONS AND TECHNOLOGIES (FORMER STATUS SEMINAR CHIP TECHNOLOGIES)

3 — 4 FEBRUARY, 2011

FRANKFURT AM MAIN, GERMANY

Contact:

DECHEMA e.V., Ms Xueqing Wu, Theodor-Heuss-Allee 25, 60486 Frankfurt am Main, Germany

Tel:+49-6975-64-152, Fax:+49-6975-64-304

Web site: <http://events.dechema.de/en/chips2011.html>